Supporting Information for

Photo-production of Reactive Oxygen Species and Degradation of Dissolved Organic Matter by Hematite Nanoplates Functionalized by Adsorbed Oxalate

Xiaopeng Huang,[*,†] *Qian Zhao,*[‡] *Robert P. Young,*[‡] *Xin Zhang,*[†] *Eric D. Walter,*[‡] *Ying Chen,*[‡] *Elias Nakouzi,*[†] *Sandra D. Taylor,*[†] *John S. Loring,*[†] *Zheming Wang,*[†] *Kirsten S. Hofmockel*[‡] and *Kevin M. Rosso*[*,†]

[†]Physical and Computational Sciences Directorate, Pacific Northwest National Laboratory, Richland, Washington 99352, United States

[‡]Environmental Molecular Sciences Laboratory, Pacific Northwest National Laboratory, Richland, Washington 99352, United States

[*]To whom correspondence should be addressed.

(K.M.R) kevin.rosso@pnnl.gov, +1-509-371-6357;

(X.H.) xiaopeng.huang@pnnl.gov, +1-509-375-6719.

Contents

Text S1. Materials. 1,10-phenanthroline, hydroxylamine hydrochloride, iron chloride, rhodamine B, sodium hydroxide, sodium chloride, ethanol (100%), hydrochloric acid (12 mol/L), oxalic acid (purified, 99.99%), 5-(diethylphosphono)-5-methyl-1-pyrroline N-oxide (DEPMPO), 5,5-Dimethyl-1-Pyrroline N-oxide (DMPO), Titanium(IV) oxysulfate-sulfuric acid (5% Ti and 27%-31% H_2SO_4), and other reagents were obtained from Sigma-Aldrich. The DMPO was purified by granular activated charcoal with 20-60 mesh. The concentration of stock solutions of DEPMPO and DMPO were both 200 mM and were maintained in a refrigerator at 4 ^oC until use in EPR measurements. Nanopure^{TM} water with a resistivity of 18.2 MΩ·cm was made by a Barnstead Nanopure Diamond water purification system and used throughout the experiments.

Text S2. Synthesis of Hematite Nanoplates. Briefly, 4.0 mM of iron chloride was dissolved in ethanol (40.0 mL) under magnetic stirring. Afterwards, Nanopure^{TM} water (2.8 mL) and sodium acetate (3.2 g) were added to dissolve it completely. The mixtures were transferred into a Teflon liner, which were then sealed and then incubated in an oven at 180 ^oC for 12 hours. After the reaction, the harvested sample was thoroughly washed with Nanopure^{TM} water and ethanol, and dried at 50 ^oC overnight.

Text S3. Characterization. The morphology and crystallinity of the hematite sample were investigated by a JEOL JSM-2010 high-resolution transmission electron microscopy (HRTEM) and high-angle annular dark-field (HADDF) scanning transmission electron microscope (STEM). Electron micrographs acquired in STEM mode were analyzed using in-house Matlab scripts to detect the surface defects. For this purpose, the images were passed through a median filter, followed by an adaptive thresholding algorithm. The objects that showed significant contrast gradients from the

neighboring pixels were assigned as defects. False and missed detections were corrected using a semi-automated tool that allows user input. For cases of stacked platelets, sharp contrast changes were ascribed to platelet boundaries, allowing us to scale the number of detected defects by the corresponding surface areas to obtain defect densities.

Text S4. Analytical Methods. Attenuated total reflectance Fourier transform infrared (ATR-FTIR) spectra were obtained with a Bruker Tensor 37 spectrometer equipped with a diamond internal reflection element (IRE) and regular deuterated triglycine sulfate (DTGS) detector. The spectra of background and sample were recorded from 5000 to 600 cm^{-1} at resolution of 4 cm^{-1} and 128 of averaged scans. Due to the negligible dissolved oxalate in the solution, the oxalate adsorbed on the hematite surface was measured. Briefly, the slurries of hematite samples after reaction were collected, separated by centrifuge and finally dried in an oven for ATR-FTIR measurement. The concentration of H_2O_2 was colorimetrically measured by Titanium(IV) oxysulfate-sulfuric acid ($TiOSO_4/H_2SO_4$) reagent.[1] Briefly, 0.1 mL of the reaction solution at regular time intervals was added to 1 mL of $TiOSO_4/H_2SO_4$ solution and analyzed from the calibration curve of pertitanic acid at 407 nm on a UV-vis spectrophotometer (UV-vis 2501PC). The fluorescence emission spectra were recorded on a Horiba Fluorolog III spectrometer.

Text S5. EPR Spectroscopy. All EPR measurements were performed on Bruker ELEXSYS E580 spectrometer equipped with an SHQE resonator with an optical access port for *in situ* illumination. A capillary with ID 0.8 mm and OD 1 mm was used to hold the solution in the EPR cavity with both ends sealed by Critoseal. The typical settings for the instrument were a microwave frequency of 9.32 GHz, 150 G sweep width in 10.5 s at a microwave power of 20 mW and 0.5 G field modulation

amplitude. Because most ROS have a short life time from nanoseconds to several seconds,[2] while after reaction with the spin trap they can last minutes to hours. Previous articles usually show a single EPR spectrum acquired about 2 minutes after the start of the reaction[3] while a series of in-situ spectra over the course of 16 minutes were recorded in current study. Additionally, the spin trap (DEPMPO) we used was much more sensitive than the traditional spin trap DMPO for measuring the ROS (the DMPO-trapped EPR spectra was also provided). For instance, DEPMPO has separate signal for hydroxyl and superoxide, DMPO does not.[4] Lifetime is ~ 20 min., DMPO is >1 min with superoxide (also much longer with hydroxyl radicals). The time dependence of the trapped signal is merely the system coming to equilibrium (i.e. when the rate of radical creation equals the rate of disappearance).

Text S6. Natural DOM Extraction. DOM was extracted from agricultural soils, which were sampled from the Great Lakes Bioenergy Research Center (GLBRC) in May 2017. Wisconsin (WI) field site is located at the Arlington Agricultural Research Station (AARS) of the University of Wisconsin-Madison (43°18' N, 89°20' W) and Michigan (MI) field site is located at the W.K. Kellogg Biological Station (KBS) Long-Term Ecological Research Site (42°24′ N, 85°24′ W), USA. The top 15 cm of soil from five replicate blocks were collected and composited. Soil was transported to the laboratory on ice packs, passed through a 2-mm sieve to remove large rocks and visible roots, and air dried at room temperature. Wisconsin soil was characterized as silty loam with (66.1±3.6)% silt (n=50), while Michigan soil was classified as sandy loam, containing (62.6±12.6)% sand (n=50).

   4 g of dry soil was weighed in polypropylene centrifuge tubes and mixed with Nanopure™ water at 1:10 w/v ratio. Tubes with soil slurry were shaken on a horizontal shaker at 100 rpm and (22±1) °C for 16 h and then centrifuged at 2800 g for 10 min. The supernatant was collected and filtered using

0.2 μm PVDF membrane syringe filters. Filters were pre-rinsed by nanopore water two times with 30 mL each time. Finally, two chromophoric dissolved organic matter samples were generated by extracting from Wisconsin soil (DOM_{WS}) and Michigan soil (DOM_{MS}), respectively. The protocols regarding the photodegradation of DOM are described in detail in Text S9 of the Supporting Information.

Text S7. FTICR MS Data Acquisition and Data Analysis. For ultrahigh resolution characterization of dissolved organic matter, the samples extracted from soil were analyzed using a 12 Tesla FTICR mass spectrometer (Bruker-SolariX) that uses an electrospray ionization (ESI) source to generate negatively charged molecular ions. The water extracts were diluted in MeOH in a 1:2 ratio to improve ESI efficiency and introduced directly to the ESI source equipped with a fused silica tube (30 μm i.d.) through an Agilent 1200 series pump (Agilent Technologies) at a flow rate of 3.0 μL/min.[5] The ion accumulation time (IAT) was varied to account for differences in carbon concentration between samples. Other experimental conditions include needle voltage at +4.4 kV; Q1 set to 50 m/z; and the heated resistively coated glass capillary operated at 180 °C. Each sample was scanned on an average of 144 scans and internally calibrated using organic matter homologous series separated by 14 Da (–CH_2 groups). The mass measurement accuracy was typically within 1 ppm. The mass resolution was 350,000 at 339.112Da. Raw spectra were converted to lists of m/z values with DataAnalysis software (BrukerDaltonics version 4.2), applying FTMS peak picker with S/N threshold set to 7 and absolute intensity threshold to the default value of 100. Chemical formulas were assigned based on the following criteria: S/N >7, and mass measurement error <1 ppm, taking into consideration the presence of C, H, O, N, S and P and excluding other elements.[6] Peaks with large mass ratios (m/z values >500 Da) were assigned formulas through propagation of CH_2, O, and H_2 homologous series.

Text S8. Nuclear Magnetic Resonance Spectroscopy. 1D ^{1}H NMR measurements were used to characterize the extracted and filtered DOM following the addition of hematite nanoparticles and oxalate including portions exposed to light irradiation and their corresponding unexposed controls. Centrifugation was used to pellet the HNPs and 7 mL of the supernatants were lyophilized to dryness and reconstituted in 100% D_2O (D, 99.96 %, Cambridge Isotope Laboratories) were transferred to 3mm NMR tubes for measurement. Additionally, 7 mL of each sample was freeze dried, reconstituted in 1.00 mL of 100% D_2O with 0.1 mM DSS-d6, and transferred to 5mm NMR tubes for measurement. Measurements were conducted using a Bruker Avance III spectrometer operating at a field strength of 17.6 T (^{1}H ν_0 of 750.24 MHz) and equipped with a 5mm Bruker TCI/CP HCN (inverse) cryoprobe. The W5 WATERGATE water suppression pulse sequence[7] was used to acquire each spectrum which consisted of a 16.0 ppm spectral window, a 1.36 second acquisition time (16k total points), followed by a 45 second relaxation delay. The binomial water suppression delay was set to 111 μs in the W5 WATERGATE pulse sequence so that the first nulls occurred outside the signal region at 10.7 and -1.3 ppm. A total of 128 transients were coadded for each spectrum and post-acquisition processing included zero-filling to 64k points, exponential multiplication (1 to 5 Hz line-broadening), and baseline subtraction of a D_2O blank acquired under identical conditions followed by a multipoint cubic spline baseline correction using MestReNova version 14.0.1. To determine the relative proportions of signals corresponding to major structural moieties, each spectrum was divided into five characteristic ^{1}H chemical shift regions (as in Hertkorn et al.[8]) and the signal intensity integrated as described further in the main body of the manuscript.

Text S9. Photodegradation Experiments. Briefly, 50 mg of hematite was added to RhB solution in

the dark. Afterwards, oxalate was added to the mixture and allowed to reach an adsorption-desorption equilibrium under magnetic stirring followed by Xenon arc lamp illumination (200 W). To avoid the temperature increase during the irradiation, the reaction was maintained under Pyrex glass jacket with circulating water. The initial concentrations of RhB and oxalate were 2×10^{-5} mol/L and 1×10^{-3} mol/L, respectively. The initial pH was regulated at 4.0±0.1. Under illumination, 1 mL of aliquot from the reaction solution was withdrawn at 30 minutes regular time intervals and subsequently analyzed with a UV-vis spectrophotometer. The photodegradation of DOM was followed using the same experimental conditions. The dissolved organic carbon (DOC) of the aliquots at regular time intervals were examined with a TOC analyzer. Noteworthily, because it was found that 0.2 μm membrane syringe completely removed the undissolved organic matter during the extraction process, the measured DOC is essentially equal to total organic carbon (TOC), and the decrease of DOC thus indicates the mineralization of DOM in the current study. Briefly, aliquots at regular time intervals were injected in the TOC analyzer and combusted afterwards. A carbon calibration curve was set up by measuring a set of standard solutions with known organic carbon concentration.

Text S10. Photodegradation of RhB. It is known that the components of natural chromophoric DOM extracted from soil are extremely complicated, containing many millions of organic molecules.[9] Under this circumstance, selecting a simple model chromophoric organic compound as a single component is a useful initial strategy. It is well documented in our previous research that RhB can be regarded as a "pseudo DOM" as it contains analogous functional groups to natural organic chromophores.[10] Degradation of RhB by hydroxyl radical occurs by electrophilic attack, forming bio-available LMW substances and inorganic species.[11] We therefore first used RhB as a proxy compound in our experiments.

With RhB added to our photodegradation system, control measurements showed that addition of hematite nanoplates alone did not lead to detectable reaction with RhB under illumination (Fig. S1A in the Supporting Information), revealing as expected that the direct photodegradation effects of hematite was negligible. The insignificant degradation of RhB by hematite alone under light can be attributed to the ultrafast charge carrier recombination time and the short hole diffusion length from associated with band gap excitation,[12, 13] consistent with our control experiments in which no Fe(II) or ROS was detected by hematite alone under illumination. Similarly, oxalate alone under light didn't induce degradation of RhB, ruling out the direct photodegradation effects of oxalate (Fig. S1A in the Supporting Information). In the combined system, however, RhB was efficiently degraded in the presence of both hematite and oxalate while under illumination (Fig. S1A in the Supporting Information). Based on the EPR measurements described above, this suggested that the observed generation of substantial amounts of hydroxyl radicals was the most likely RhB degradation mechanism. We confirmed this by adding selective scavengers to the combined illuminated system. For example, the addition of ethanol, which scavenges ROS and high-valent iron-oxo complex in the Fenton process, significantly decreased the degradation rate of RhB (Fig. S1B in the Supporting Information), reinforcing the conclusion that RhB is likely oxidized by ROS. Addition of iso-propanol, a scavenger selective for hydroxyl radicals ($k = 1.9 \times 10^9$ L mol^{-1} s^{-1}),[14] decreases the rate of RhB degradation equally well (Fig. S1B in the Supporting Information), confirming that the most likely ROS species responsible for RhB degradation was hydroxyl radical. It is noteworthy that the scavenger experiments cannot be conducted along with the DOM degradation in a straightforward manner, because characterization of the DOM would then become convoluted with unknown effects of the scavengers themselves.

Text S11. DOM characterizations. Both DOM_{WS} and DOM_{MS} samples were visibly light colored (inserted in Fig. S2A), a typical characteristic of chromophoric DOM. The original DOC values were 138.4 and 220.1 mg/L for DOM_{WS} and DOM_{MS}, respectively. UV-vis measurements of the dissolved fractions showed an approximately exponential decrease in absorption intensity with an increase in wavenumber (see Fig. S2A) and the stronger absorption in the UV region indicates the presence of aromatic or other organic chromophores as has been cited in other studies.[15] The higher intensity of DOM_{WS} than DOM_{MS} in the spectra indicated that DOM_{WS} contains more chromophores even though DOM_{WS} has a lower DOC concentration.

FTICR-MS spectra showed the enormous numbers of organic molecules contained in the two DOM samples, predominantly distributed from 200 to 700 m/z in abundance (top Fig. S2B), indicative of the molecular diversity within environmental samples, including aromatic carbon (lignin and condensed hydrocarbons) and aliphatic carbon (proteins, lipids, and amino sugars), etc. The magnified region of FTICR-MS spectra showed noteworthy differences in organic molecule content between the two DOM (bottom Fig. S2B). For instance, peaks at 383.04, 383.18, and 383.19 can be assigned as condensed hydrocarbon-, lipid-, and amino sugar-like molecules, indicating that these molecules are present in DOM_{WS} but not in DOM_{MS}.
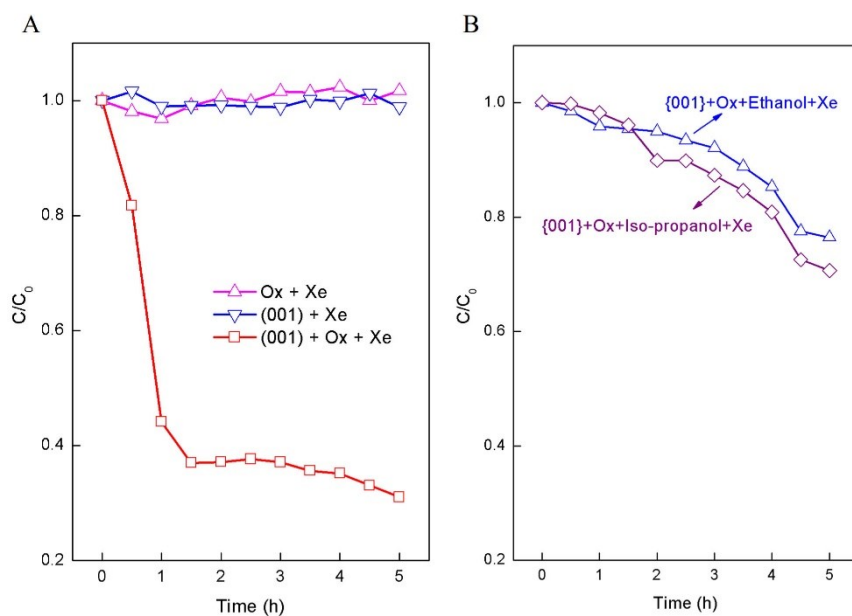
Figure S1. (A) Photodegradation of RhB in the presence of hematite and oxalate under light illumination. (B) Scavenger experiments in the degradation of RhB in the presence of hematite nanoplates and hydrogen peroxide under light illumination.
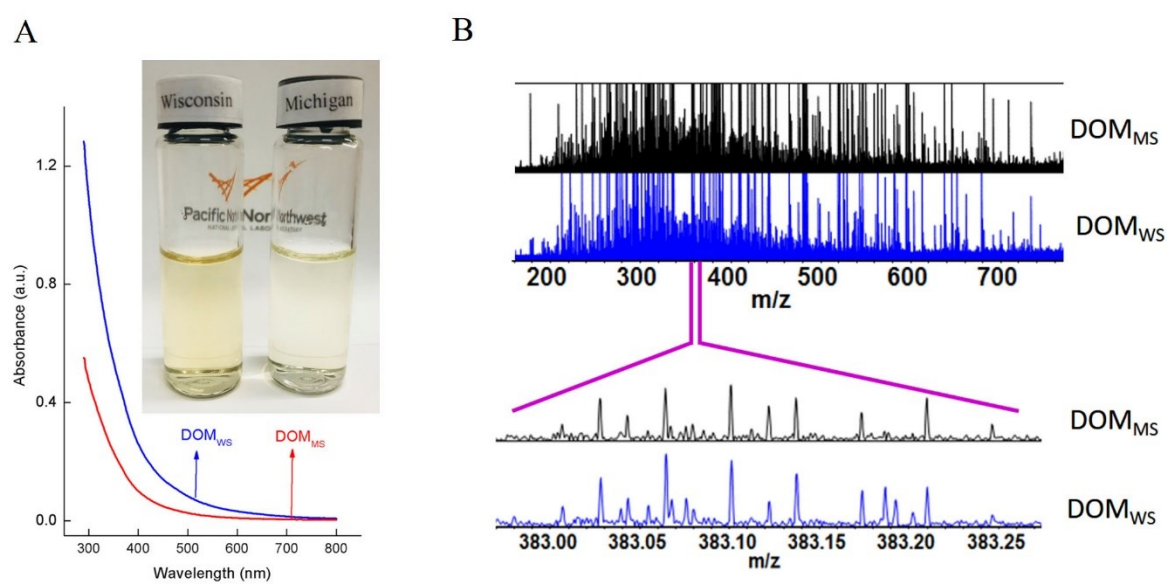
Figure S2. Characterization of pristine dissolved organic matter solutions. (A) UV-vis absorption spectra of the DOM and the corresponding pictures (insert). (B) FTICR-MS spectra (top) and its magnified reign (bottom).
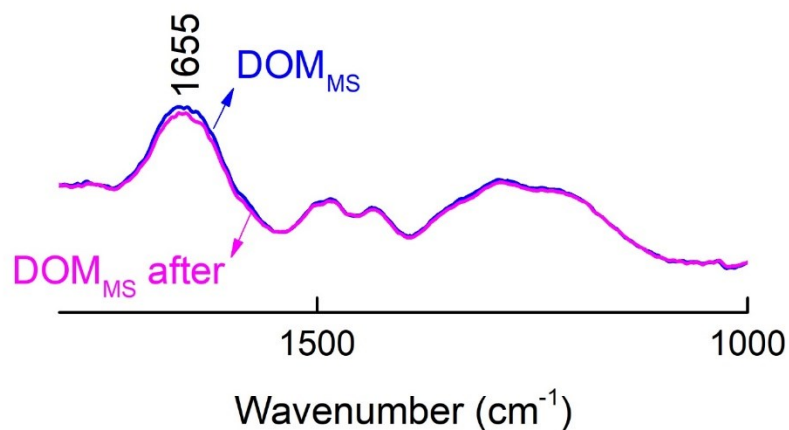
Figure S3. The magnified ATR-FTIR spectra of the DOM_{MS} before and after the photoreaction in 1800-1000 cm^{-1}. The distinguished peak at 1655 cm^{-1} was attributed to the aromatic C=C and/or amide C=O functional groups.

Table S1. Defects of hematite (001) and (012) facet change before and after the photochemical reaction using TEM and STEM characterizations.

image type	plane	reaction	defect area (%)	average defect size (nm^2)	defect density (defect/nm^2)
TEM	(001)	before	NA	NA	NA
TEM	(001)	after	2.44	0.1434	2.19×10^{-4}
STEM	(001)	before	0.40	0.0225	0.50×10^{-4}
STEM	(001)	after	2.55	0.0608	2.31×10^{-4}
STEM	(012)	before	0.19	0.0382	0.018×10^{-4}
STEM	(012)	after	0.17	0.0236	0.021×10^{-4}

References

1. I. R. Cohen, T. C. Purcell and A. P. Altshuller, Analysis of the oxidant in photooxidation reactions, *Environ. Sci. Technol.*, 1967, **1**, 247-252.

2. W. A. Pryor, Oxy-Radicals and Related Species: Their Formation, Lifetimes, and Reactions, *Annu. Rev. Physiol.*, 1986, **48**, 657-667.

3. X. Huang, X. Hou, F. Jia, F. Song, J. Zhao and L. Zhang, Ascorbate-promoted surface iron cycle for efficient heterogeneous Fenton alachlor degradation with hematite nanocrystals, *ACS Appl. Mater. Interfaces*, 2017, **9**, 8751-8758.

4. C. Frejaville, H. Karoui, B. Tuccio, F. le Moigne, M. Culcasi, S. Pietri, R. Lauricella and P. Tordo, 5-Diethoxyphosphoryl-5-methyl-1-pyrroline N-oxide (DEPMPO): a new phosphorylated nitrone for the efficient In Vitro and In Vivo spin trapping of oxygen-centred radicals, *J. Chem. Soc., Chem. Commun.*, 1994, DOI: 10.1039/C39940001793, 1793-1794.

5. M. M. Tfaily, R. K. Chu, N. Tolić, K. M. Roscioli, C. R. Anderton, L. Paša-Tolić, E. W. Robinson and N. J. Hess, Advanced Solvent Based Methods for Molecular Characterization of Soil Organic Matter by High-Resolution Mass Spectrometry, *Anal. Chem.*, 2015, **87**, 5206-5215.

6. E. B. Kujawinski and M. D. Behn, Automated Analysis of Electrospray Ionization Fourier Transform Ion Cyclotron Resonance Mass Spectra of Natural Organic Matter, *Anal. Chem.*, 2006, **78**, 4363-4373.

7. M. Liu, X.-a. Mao, C. Ye, H. Huang, J. K. Nicholson and J. C. Lindon, Improved WATERGATE Pulse Sequences for Solvent Suppression in NMR Spectroscopy, *J. Magn. Reson.*, 1998, **132**, 125-129.

8. N. Hertkorn, M. Harir, B. Koch, B. Michalke and P. Schmitt-Kopplin, High-field NMR

spectroscopy and FTICR mass spectrometry: powerful discovery tools for the molecular level characterization of marine dissolved organic matter, *Biogeosciences*, 2013, **10**, 1583-1624.

9. G. R. Aiken, H. Hsu-Kim and J. N. Ryan, Influence of Dissolved Organic Matter on the Environmental Fate of Metals, Nanoparticles, and Colloids, *Environ. Sci. Technol.*, 2011, **45**, 3196-3201.

10. X. Huang, Y. Chen, E. Walter, M. Zong, Y. Wang, X. Zhang, O. Qafoku, Z. Wang and K. M. Rosso, Facet-Specific Photocatalytic Degradation of Organics by Heterogeneous Fenton Chemistry on Hematite Nanoparticles, *Environ. Sci. Technol.*, 2019, **53**, 10197-10207.

11. X. Huang, X. Hou, J. Zhao and L. Zhang, Hematite facet confined ferrous ions as high efficient Fenton catalysts to degrade organic contaminants by lowering H_2O_2 decomposition energetic span, *Appl. Catal., B*, 2016, **181**, 127-137.

12. D. A. Wheeler, G. M. Wang, Y. C. Ling, Y. Li and J. Z. Zhang, Nanostructured hematite: synthesis, characterization, charge carrier dynamics, and photoelectrochemical properties, *Energy Environ. Sci.*, 2012, **5**, 6682-6702.

13. J. Deng, X. Lv, J. Gao, A. Pu, M. Li, X. Sun and J. Zhong, Facile synthesis of carbon-coated hematite nanostructures for solar water splitting, *Energy Environ. Sci.*, 2013, **6**, 1965-1970.

14. G. V. Buxton, C. L. Greenstock, W. P. Helman and A. B. Ross, Critical Review of rate constants for reactions of hydrated electrons, hydrogen atoms and hydroxyl radicals ($\bullet OH/\bullet O^-$) in Aqueous Solution, *J. Phys. Chem. Ref. Data*, 1988, **17**, 513-886.

15. J. Chen, B. Gu, E. J. LeBoeuf, H. Pan and S. Dai, Spectroscopic characterization of the structural and functional properties of natural organic matter fractions, *Chemosphere*, 2002, **48**, 59-68.